Available online at www.sciencedirect.com
ScienceDirect
Carbohydrate Polymers 71 (2008) 196–207
Carbohydrate Polymers
www.elsevier.com/locate/carbpol

Ultra-fine cellulose acetate/poly(ethylene oxide) bicomponent fibers

Lifeng Zhang, You-Lo Hsieh *

Fiber and Polymer Science, University of California, Davis, CA 95616, USA

Received 16 March 2007; received in revised form 17 May 2007; accepted 22 May 2007
Available online 2 June 2007

Abstract

Formation of cellulose acetate (CA) and poly(ethylene oxide) (PEO) bicomponent fibers by electrospinning of binary mixtures of these polymers was strongly influenced by their chain lengths, concentrations and mixed ratios as well as the solvents employed. Individually, the threshold molecular weights that supported fiber generation were 50 kDa and 100 kDa for CA and PEO, respectively. Adding dioxane, a lower dielectric constant co-solvent, enabled fiber formation from CA alone at a lower 30 kDa as well as from binary systems with one low molecular weight polymer that was not fiber forming. While bicomponent fiber formation generally improved with longer polymers and higher concentrations, fiber sizes also increased with both these factors. PEO in the bicomponent fibers was clearly phase-separated and the phase separation of long chains was facilitated by DMF, whereas that of shorter chains by DMF/dioxane. A phase-separated CA core and PEO sheath structure of the bicomponent fibers was strongly supported by experimental evidence.

Keywords: Cellulose acetate; Poly(ethylene oxide); Bicomponent fiber; Electrospinning; Molecular weight; Phase separation; Sheath–core structure

1. Introduction

Electrospinning of polymer solutions or melts to generate sub-micrometer diameter fibers has been extensively reported since the resurgence of interest in the 1990's (Doshi & Reneker, 1995). Most have focused on fiber formation from single polymer systems to study the electrospinning conditions and variables (Demir, Yilgor, Yilgor, & Erman, 2002), the theoretical modeling of the process (Subbiah, Bhat, Tock, Parameswaran, & Ramkumar, 2005) and the use of new polymers (Reneker & Chun, 1996) or natural polymers, such as proteins (Xie & Hsieh, 2003) and polysaccharides (Li & Hsieh, 2006) that cannot be electrospun into fibers alone. Some recent attention has been directed toward electrospinning of dual- or multi-component polymer systems to produce fibers with novel properties and structures. For instance, new hydrogel fibers were electrospun from aqueous mixtures of polyacrylic acid and polyvinyl alcohol followed by crosslinking (Li & Hsieh, 2005a, 2005b) and conductive fibers were produced from mixing polyaniline with gelatin (Li, Guo, Wei, MacDiarmid, & Lelkes, 2006). Fibers with sheath–core structure were electrospun from poly(ethylene oxide) (PEO) with either polysulfone or poly(dodecylthiophene) as well as from poly(L-lactide) and $Pd(OAc)_2$ with coaxial dual-capillary spinnerets (Sun, Zussman, Yarin, Wendorff, & Greiner, 2003). Our lab has successfully demonstrated that phase separation, a well-known behavior of polymer mixtures (Folkes & Hope, 1993; Creton, Kramer, & Hadziioannou, 1991; Inoue, Ougizawa, Yasuda, & Miyasaka, 1985), could be utilized to generate bicomponent fibers with nanoporous structures (Zhang & Hsieh, 2006). Selective dissolution of the phase-separated PEO domains in electrospun bicomponent fibers from polyacrylonitrile (PAN) and PEO in *N*,*N*-dimethylformamide (DMF) resulted in nanoporous PAN fibers with 130 nm average pore diameter, 50% higher pore volume and 2.5-fold higher specific surface. Electrospinning of the PAN–PEO pair showed an island-in-the-sea phase-separated structure in the fibers.

This study was to investigate generation of cellulose-based bicomponent fibers by electrospinning of binary mix-

* Corresponding author. Tel.: +1 530 752 0843; fax: +1 530 752 0843.
E-mail address: ylhsieh@ucdavis.edu (Y.-L. Hsieh).

0144-8617/$ - see front matter © 2007 Elsevier Ltd. All rights reserved.
doi:10.1016/j.carbpol.2007.05.031

ture with PEO. The flexible chain structure and ease of crystallization of PEO are expected to facilitate its separation from the more rigid and bulky cellulose molecules. Cellulose acetate (CA) was chosen for its ease of solubility in place of cellulose whose dissolution requires the use of special solvents, such as *N*-methylmorpholine-*N*-oxide/water (Kulpinski, 2005) or lithium chloride/*N*,*N*-dimethylacetamide (DMAc) (Kim, Frey, Marquez, & Joo, 2005). Not only CA could be easily electrospun into fibers of varying sizes and packing structures, the ultra-fine fibers could be converted to pure cellulose by aqueous or ethanolic hydrolysis (Liu & Hsieh, 2002). Several mixtures of three common solvents for CA, i.e., acetone, acetic acid and DMAc, enabled continuous electrospinning into fibers, although none alone could support fiber formation. The 2:1 acetone/DMAc mixture was found to be particularly versatile and efficient in generating CA fibers at concentrations between 10 and 20% (Liu & Hsieh, 2002; Ding, Kimura, Sato, Fujita, & Shiratori, 2004). Other reported solvents involved in the electrospinning of CA were acetone/water (80:20, w/w) (Son, Youk, Lee, & Park, 2004a). To make CA and PEO binary solutions, a common solvent that is also amenable to electrospinning is needed. DMF was selected as the common solvent because of its high dielectric constant and boiling point, both favorable for electrospinning. DMF has shown to be the most favorable solvent for electrospinning of thin PEO fibers (Son, Youk, Lee, & Park, 2004b). The low evaporating rate of DMF prevents blockage and facilitates continuity of electrospinning. The objective of this paper was to study the impact of polymer molecular weight, concentration, mixing composition as well as the solvent systems in the formation of bicomponent fibers. The phase-separation behavior of the two polymer components in fibers were studied for its potential in generating bio-based fibers with special morphology such as porous, hollow or sheath–core structures.

2. Experimental

2.1. Materials

Cellulose acetate (CA) (Mn = 30 kDa, degree of substitution or DS = 2.45) and poly(ethylene oxide) (PEO) (Mn = 10, 100 and 600 kDa) were purchased from Aldrich Chemical Company Inc. CA (Mn = 40, 50 and 60 kDa, DS = 2.45) was provided by Eastman Chemical Company. *N*,*N*-dimethylformamide (DMF) and dioxane were purchased from EMD Chemicals Inc. All materials and solvents were used as received.

2.2. Procedures

Homogeneous solutions of CA, PEO and their mixtures were prepared in DMF or 1:1 DMF/dioxane mixture under constant stirring at 40 °C. All solution concentrations reported were weight percentages. The total polymer concentrations were between 5% and 30% and the CA/PEO compositions were varied at 70/30, 50/50 and 30/70 mass ratio. The viscosities of 20% CA solutions in DMF and 1:1 DMF/dioxane as well as PEO (100 kDa) solutions in DMF from 1% to 20% were measured at 40 °C using Cannon-Fenske routine viscometers according to ASTM method D445.

Electrospinning of each solution was conducted at potentials ranged from 8 to 15 kV and under ambient temperature with a previously established setup (Liu & Hsieh, 2002). An aluminum collector was grounded and placed 8 inches from the electrospinning tip. The fibrous membranes collected were dried under vacuum at ambient temperature for 24 h. For dissolution of PEO, fibrous membranes were detached from the aluminum collector and immersed into 40 °C distilled water for 4–8 h. The treated samples were then dried at 60–70 °C for at least 4 h.

2.3. Characterization

The morphology of electrospun fibers and membranes were examined by a scanning electron microscope (SEM, Philips, FEI XL30s FEG) and a transmission electron microscope (TEM, Philips, CM120). All SEM samples were sputter coated with gold. The average fiber diameters were determined by 30–50 measurements from SEM images using analysis® pro software from Soft Imaging System GmbH. For TEM examinations, the bicomponent fibers were dispersed ultrasonically in *n*-hexane for the as-spun and in water for the water-treated and collected on lacey copper grid. The thermal properties of electrospun fibers were measured in N_2 at a 10 °C/min heating rate from 30 °C to 500 °C using a Shimadzu DSC-60 differential scanning calorimeter (DSC). FT-IR spectroscopic measurements were performed on KBr pellets of samples using Nicolet Magna-IR 560 spectrometer.

3. Results and discussion

3.1. Formation of single component fibers

Electrospinning of CA at several molecular weights from 30 kDa to 60 kDa in DMF at 20% concentration produced continuous jets. Untra-fine fibers of 50–200 nm diameters were generated from CA at 50 kDa and 60 kDa (Fig. 1a and b). The electrospun products of the 30 kDa CA consisted mainly clustered beads of 200 nm–1.5 μm diameters interspersed with few 20–40 nm size fibers (Fig. 1c) while those of the 40 kDa CA contained more fibers as well as smaller beads. Adding dioxane as an equal mass co-solvent enabled formation of 200 nm diameter fibers from 30 kDa CA (Fig. 1d), although dioxane as a lone solvent could not support fiber generation. The extremely low dielectric constant of dioxane (2.2 at 20 °C) in comparison to DMF (38.3 at 20 °C) (Brandrup, Immergut, & Grulke, 1999) appears insufficient to generate the necessary force to draw out the CA solutions. However, replacing half of DMF with dioxane helped to sustain the

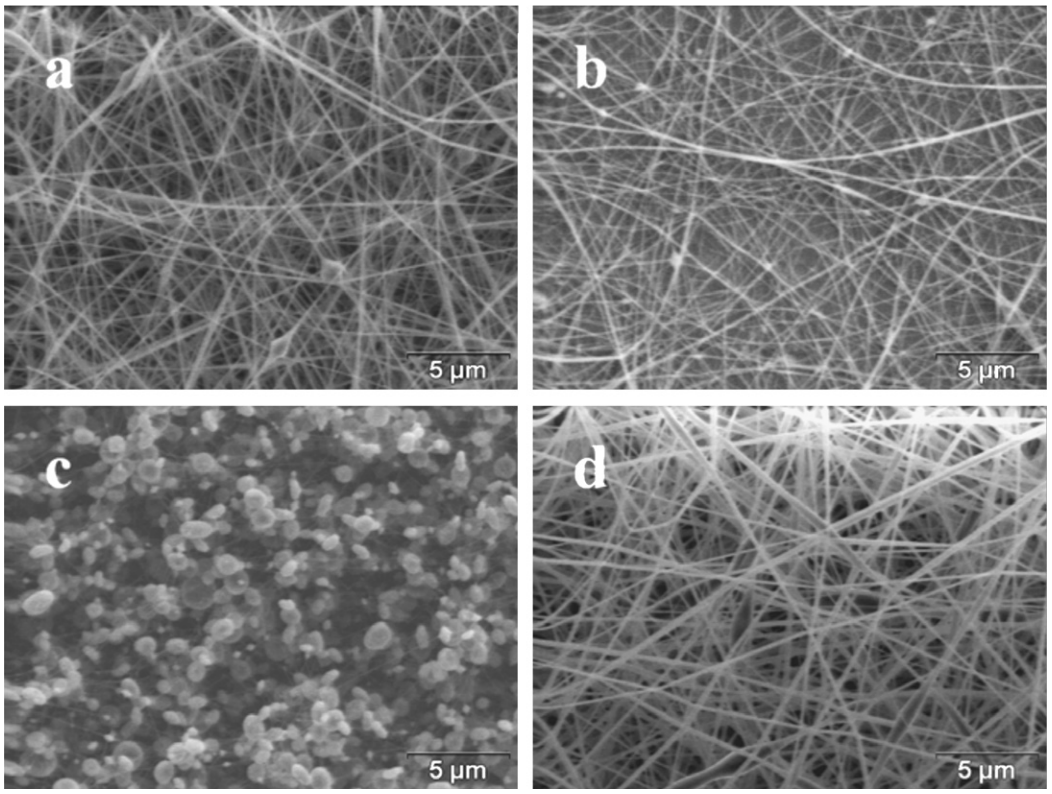

Fig. 1. CA fibers from 20% solutions (SEM, 5 μm bar): (a) 50 kDa in DMF; (b) 60 kDa in DMF; (c) 30 kDa in DMF; (d) 30 kDa in 1:1 DMF/dioxane.

continuous jet of the shorter CA chains in electrospinning, possibly due to its lowering effect on driving force.

For 20% CA solutions in either DMF or 1:1 DMF/dioxane, the log–log plots of specific viscosity (η_{sp}) showed linear relationships with the molecular weights (M) (Fig. 2). The linear regressions gave Log $\eta_{sp} = 3.38$ Log $M - 1.47$ ($r = 0.9985$) for solutions with the mixed solvent and Log $\eta_{sp} = 3.10$ Log $M - 1.16$ ($r = 0.9984$) for those in DMF. Thus, η_{sp} was proportional to $M^{3.38}$ in 1:1 DMF/dioxane and $M^{3.10}$ in DMF, indicating the dependence of specific viscosity on molecular chain length was higher in DMF/dioxane mixture than in DMF. This suggests greater molecular entanglement in the mixed solvent. That fibers could be electrospun from the shorter 30 kDa CA in 1:1 DMF/dioxane but not from DMF suggests that the positive effects of dioxane include moderation in solution conductivity and increased chain entanglement.

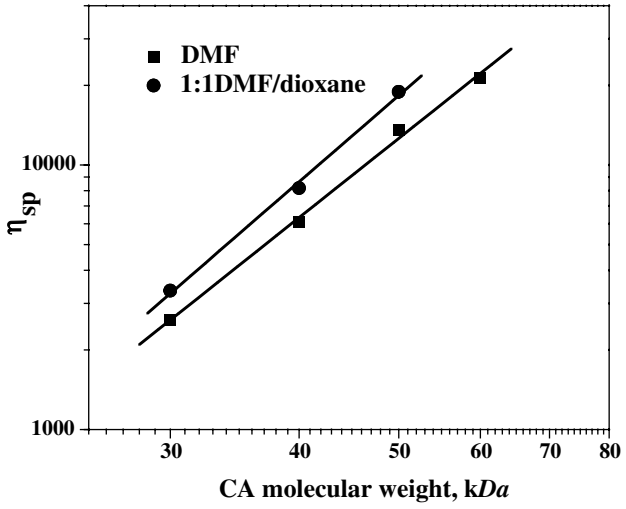

Fig. 2. Solution specific viscosity and molecular weight relationships of CA solutions.

Electrospinning of either 100 kDa PEO at 20% or 600 kDa PEO at 5% concentration was continuous and produced fibers (Fig. 3). However, the 10 kDa PEO was not fiber-forming in either DMF or DMF/dioxane mixture, even at a very high concentration of 40%. The 10 kDa PEO molecules appear to be too short to reach the extent of chain entanglement needed for fiber formation. The fibers electrospun from 100 kDa PEO in either DMF (Fig. 3a) or 1:1 DMF/dioxane mixture (Fig. 3b) were highly irregular in sizes. Fibers generated from the mixed solvent were also much larger (200 nm–3 μm) than those electrospun from DMF (40–400 nm). Fiber formation from 600 kDa PEO was possible at a much lower concentration of 5% (Fig. 3c). The fibers were straight and uniform, with the larger ones averaging around 450 nm in diameter and the smaller ones at diameters close to 100 nm.

The log–log plot of η_{sp} of 100 kDa PEO showed two increases in slopes with increasing concentration, i.e., a significant increase at just above 3% and a second slight increase at 12%, separating the viscosities into three regions (Fig. 4). The linear regressions of the data in the <3%,

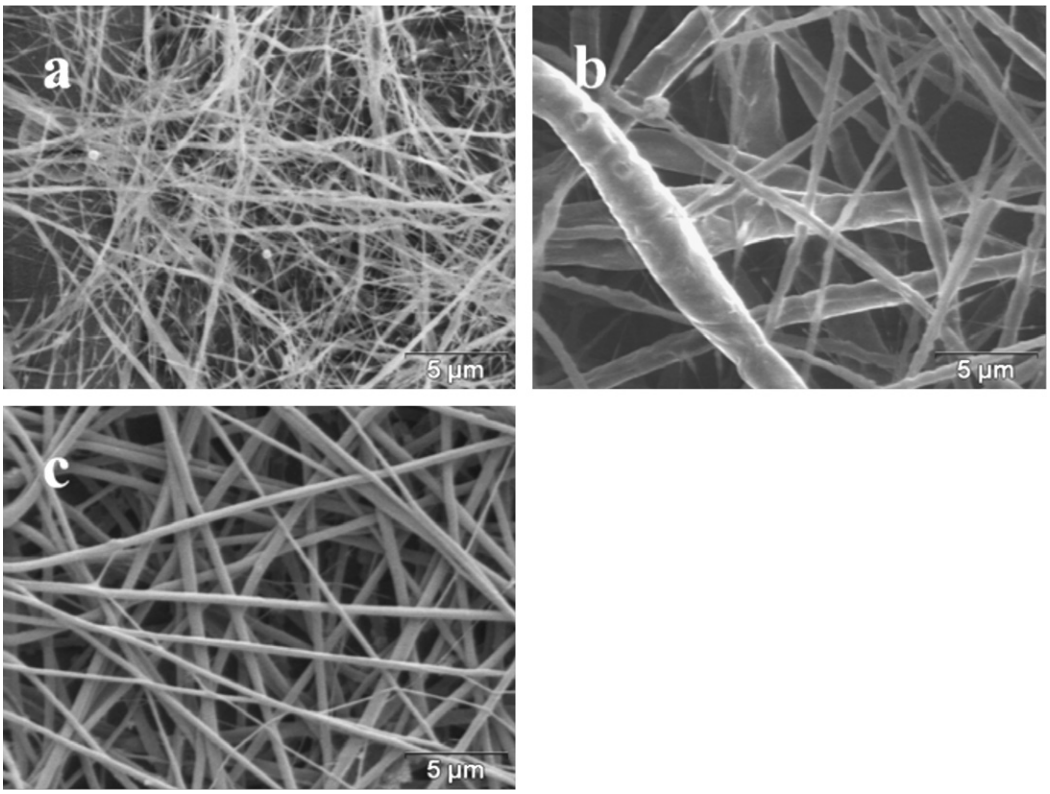

Fig. 3. PEO fibers from solutions (SEM, 5 μm bar): (a) 100 kDa in 20% DMF; (b) 100 kDa in 20% 1:1 DMF/dioxane; (c) 600 kDa in 5% DMF.

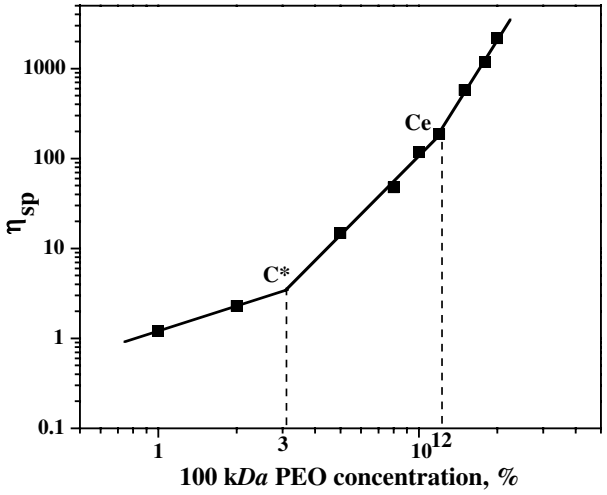

Fig. 4. Dependence of solution specific viscosity on concentration for 100 kDa PEO in DMF.

3–12% and >12% regions gave Log $\eta = 0.94$ Log $C + 0.079$, Log $\eta_{sp} = 2.94$ Log $C - 0.91$ ($r = 0.9953$), and Log $\eta_{sp} = 4.54$ Log $C - 2.59$ ($r = 0.9942$), respectively. Thus, η_{sp} was proportional to $C^{0.94}$, $C^{2.94}$ and $C^{4.54}$ in the <3%, 3–12% and >12% regions, respectively. Based on the observation that 100 kDa PEO became fiber-forming at 12% (Fig. 5), this concentration was assigned to be the starting concentration for molecular entanglement (C_e) of this PEO (Zhang & Hsieh, 2006; McKee, Wilkes, Colby, & Long, 2004).

These above data showed that the threshold molecular weights that support fiber formations from electrospinning of 20% solutions in DMF were 50 kDa and 100 kDa for CA and PEO, respectively. More importantly, adding a low dielectric constant solvent, dioxane, to DMF enabled electrospinning of CA at a lower molecular weight of 30 kDa into uniform fibers. Our previous work has shown that the 2:1 acetone/DMAc mixture was a versatile solvent system to afford highly efficient fiber generation from 30 kDa CA at a wide range of concentrations (12.5–20%, Liu & Hsieh, 2002). At the same 20% concentration, the CA fibers electrospun from the 2:1 acetone/DMAc mixture had diameters ranged from 0.83 μm to 2.5 μm, whereas those electrospun from the 1:1 DMF/dioxane mixture were much smaller, i.e., 50–200 nm. This significant reduction in fiber sizes demonstrates the critical role of solvents in fiber structure generated by electrospinning. In the case with CA, these effects may be due to a combination of the high dielectric constant of DMF and the improved compatibility of dioxane with CA.

3.2. Formation of CA/PEO bicomponent fibers

3.2.1. Co-solvent effects

Electrospinning of all CA/PEO mixtures in DMF produced jets, but fibers were not observed in every case. The lowest molecular weight pair, i.e., 30 kDa CA and 10 kDa PEO, produced only beads, attributing to the insufficient entanglement to sustain continuous polymer jet

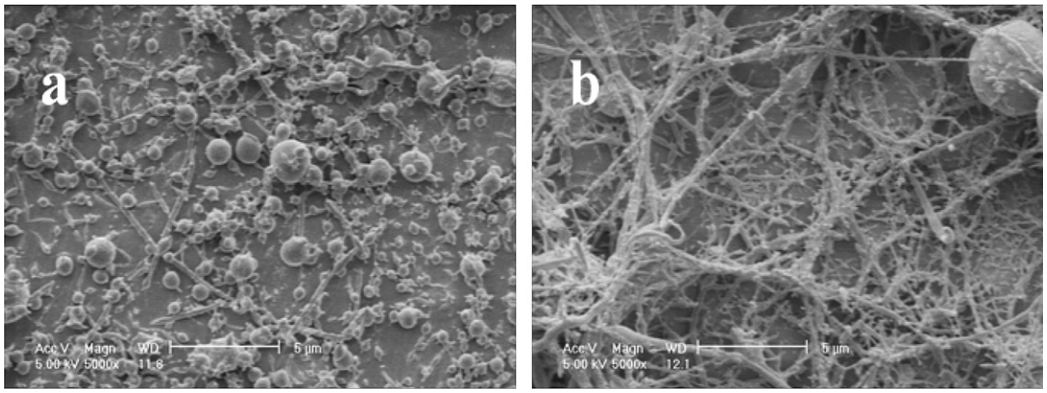

Fig. 5. PEO (100 kDa) fibers from DMF solutions (SEM, 5 μm bar): (a) 12%; (b) 15%.

under the high stretching force in DMF. Even incorporating equal mass of the fiber-forming 60 kDa CA with the non-fiber-forming 10 kDa PEO in DMF resulted in mostly beads (Fig. 6a). Adding dioxane, however, enabled generation of homogeneous bicomponent fibers (Fig. 6b), similar to the earlier observation made on the 30 kDa CA. The co-solvent, however, also produced significantly larger fibers, as observed on other equal mixtures of CA/PEO (Table 1). Therefore, in cases where high molecular weight CA and/or PEO and sufficient molecular entanglement enable continuous jet and fiber formation, dioxane addition led to enlarged fibers, another indication of reduced stretching force.

Table 1
Co-solvent effects on 50/50 CA/PEO bicomponent fiber sizes

CA (kDa)	PEO (kDa)	Concentration (%)	Average fiber sizes (nm)	
			DMF	1:1 DMF/dioxane
30	100	20	190	440
30	600	10	520	690
60	600	8	480	610

3.2.2. Molecular weight effects

The effects of molecular weight on fiber formation were studied first with the non-fiber-forming 10 kDa PEO in combination with CA of varied chain lengths. Although the 30 kDa CA was fiber-forming from 1:1 DMF/dioxane, equal mix with the non-fiber-forming 10 kDa PEO led to mostly clustered beads in wide ranging sizes (300 nm to 3 μm, Fig. 7a). With the 40 kDa CA, the electrospun products consisted smaller beads (~900 nm) interconnected with fibers (Fig. 7b). Further increasing CA to 50 kDa and 60 kDa, homogeneous fibers (average diameter 170 nm) with scarcely any beads were produced (Figs. 7c and 6b). Therefore, the threshold CA molecular weight for uniform fiber formation with equal mass of 10 kDa PEO from 1:1 DMF/dioxane solution is 50 kDa. The finding shows that bicomponent fibers can be generated from the non-fiber-forming PEO in combination with CA whose molecular weight nearly doubles that of the fiber-forming chain length when used alone.

When each component is fiber-forming, electrospinning of their mixtures is expected to be fiber forming. Indeed, generation of bicomponent fibers were observed with 30 kDa CA mixed with PEO at either 100 kDa (Fig. 8a) or 600 kDa (Fig. 8b). The longer PEO (600 kDa) could afford fibers at a much lower total polymer concentration, i.e., 10%, while yielding larger fibers, 690 nm diameter, comparing to the 440 nm diameter from the 100 kDa PEO fibers. Similarly, mixing 60 kDa CA with 600 kDa PEO lowered the fiber-forming concentration to 8% when

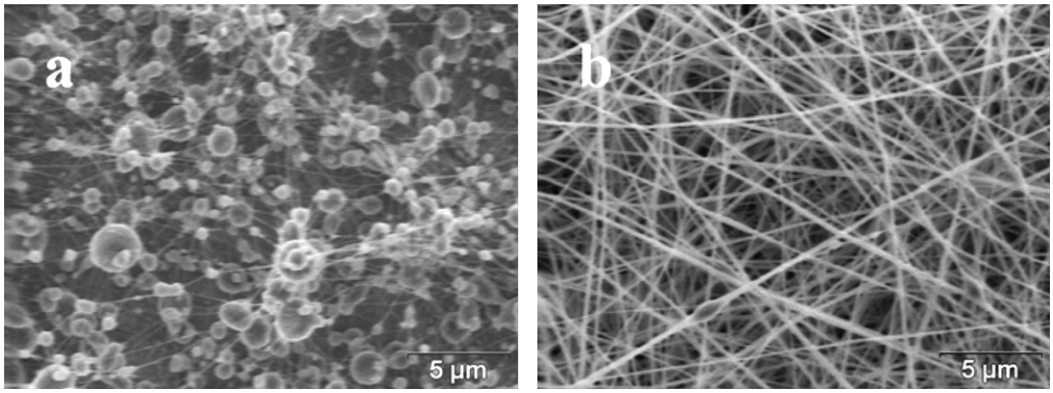

Fig. 6. Co-solvent effects on the fiber formation of 50/50 CA (60 kDa)/PEO (10 kDa) 20% solutions (SEM, 5 μm bar): (a) DMF; (b) 1:1 DMF/dioxane.

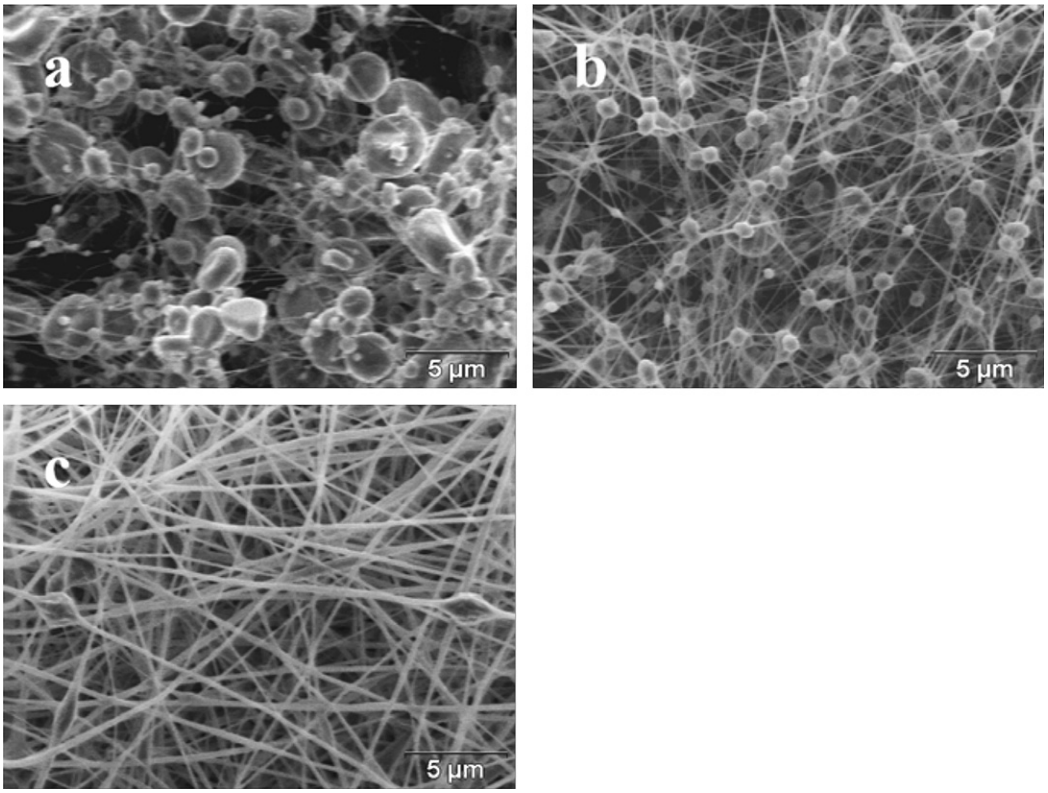

Fig. 7. CA molecular weight effects on the fiber formation of 50/50 CA/PEO (10 kDa) 20% 1:1 DMF/dioxane solutions (SEM, 5 μm bar): (a) 30 kDa; (b) 40 kDa; (c) 50 kDa.

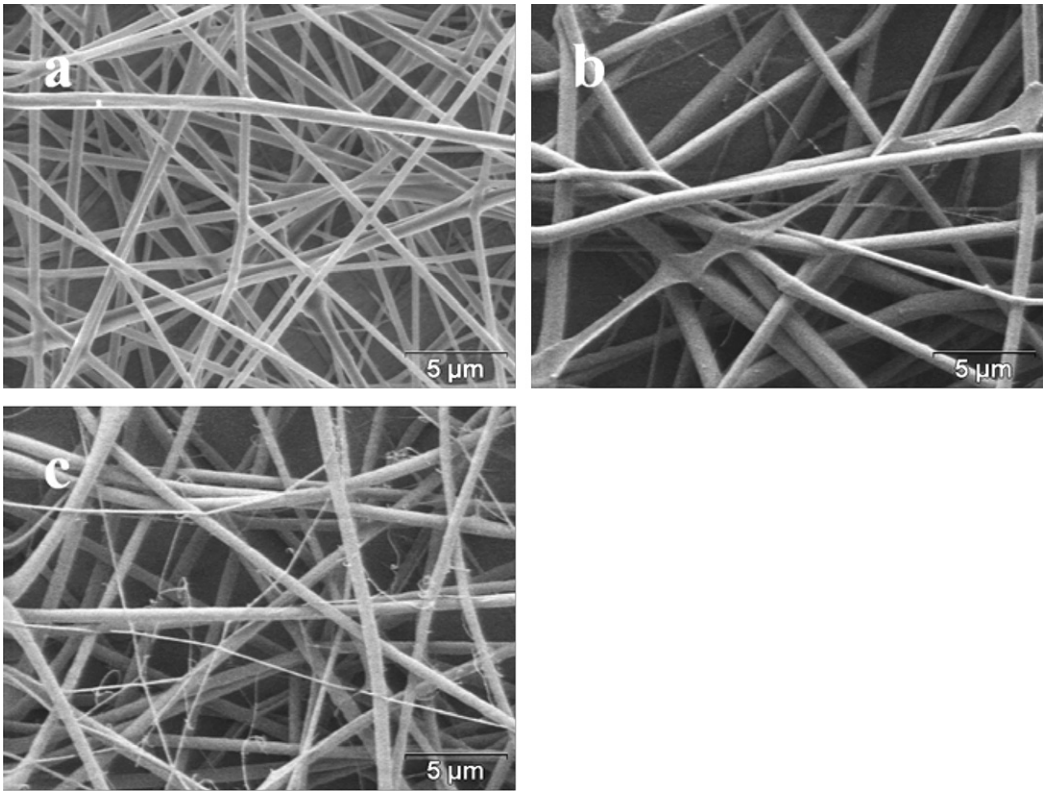

Fig. 8. PEO molecular weight effects on the fiber formation of 50/50 binary solutions in 1:1 DMF/dioxane (SEM, 5 μm bar): (a) CA (30 kDa)/PEO (100 kDa), 20%; (b) CA (30 kDa)/PEO (600 kDa), 10%; (c) CA (60 kDa)/PEO (600 kDa), 8%.

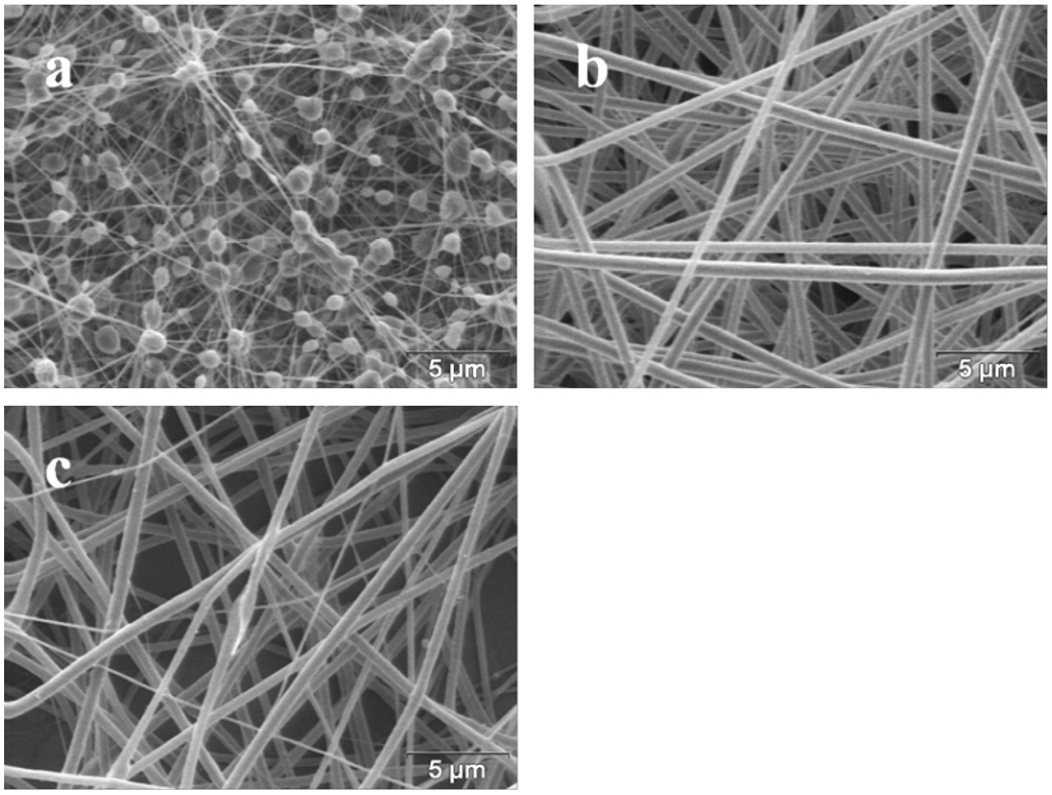

Fig. 9. Compositional effects on the fiber formation of CA (60 kDa)/PEO solutions (SEM, 5 μm bar): (a) 30/70 CA/PEO (10 kDa), 20% 1:1 DMF/dioxane; (b) 50/50 CA/PEO (600 kDa), 8% DMF; (c) 30/70 CA/PEO (600 kDa), 8% DMF.

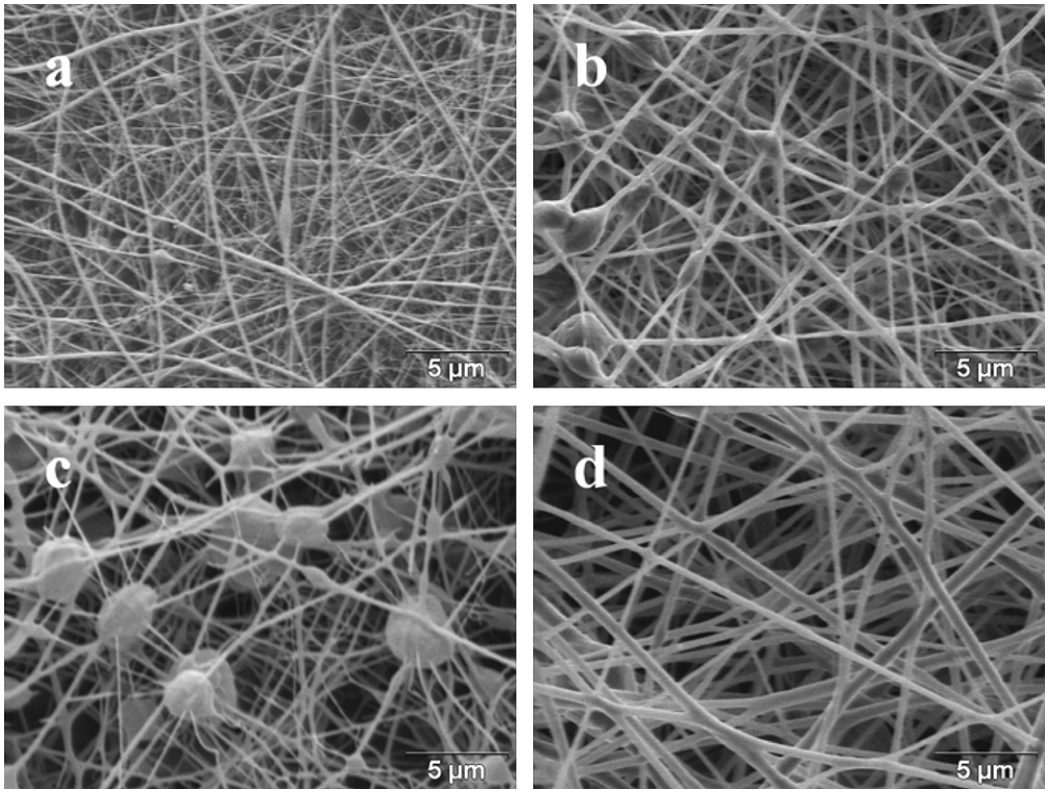

Fig. 10. Polymer concentration effects on the fiber formation from binary solutions (SEM, 5 μm bar): 50/50 CA (60 kDa)/PEO (10 kDa), 30% DMF (a); 30/70 CA (60 kDa)/PEO (10 kDa), 25% 1:1 DMF/dioxane (b); 50/50 CA (30 kDa)/PEO (100 kDa) 1:1 DMF/dioxane (c); 10%; (d) 15%.

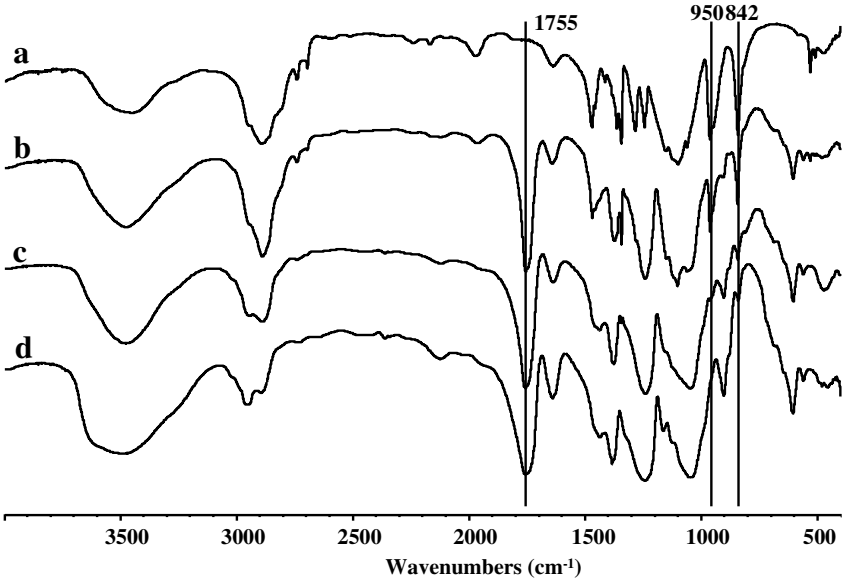

Fig. 11. FT-IR KBr spectra of 30/70 CA (60 kDa)/PEO (600 kDa) fibers from 8% DMF solution: (a) PEO fibers from 5% DMF; (b) as-spun; (c) water treated (40 °C for 4 h, weight loss was 66.1%); (d) CA fibers from 20% DMF.

compared with the 20% mixture with 10 kDa PEO. Again, larger fibers (610 nm versus 140 nm, Figs. 6b and 8c) were produced with the longer PEO, even at a lower concentration. These results showed that longer chain lengths of either polymer enabled bicomponent fiber formation at lower total polymer concentrations, but led to larger fiber sizes. With regard to the proportions of non-fiber-forming PEO (10 kDa) in mixture, reducing its proportion is necessary for bicomponent fiber formation (Figs. 6b and 9c), while increasing the proportion of fiber-forming PEO (600 kDa) had little effects (Fig. 9b and c).

3.2.3. Concentration effects

Increasing overall polymer concentrations in solution generally improved fiber formation. For the equal mass mixtures of CA (60 kDa) and PEO (10 kDa) in DMF was fiber-forming at 30% (Fig. 10a) but not at 20% (Fig. 6a). Another example was the equal mix of 30 kDa CA and 100 kDa PEO in 1:1 DMF/dioxane that formed uniform fibers at 15% (Fig. 10d) and 20% (Fig. 8a), but with large beads at 10% (Fig. 10c). Similarly, increasing the concentration of 30/70 CA (60 kDa)/PEO (10 kDa) from 20% to 25% in 1:1 DMF/dioxane greatly improved fiber formation (Figs. 9a and 10b). The fiber average sizes also significantly increased with concentrations, i.e., from 210 nm at 10% to 360 nm and 440 nm at 15% and 20%, respectively. All the above results showed that higher polymer concentrations led to more uniform, but larger fibers.

In electrospinning of either single component or bicomponent systems, longer polymer chains, higher polymer concentration and lower proportion of short polymer chains all contributed to polymer–polymer entanglement in solution, then supported continuous polymer jets and improved fibers formation. This enhanced polymer chain interaction also increased resistance to the stretching force, leading to larger fibers.

3.3. Phase separation in bicomponent fibers

The phase-separation behavior of CA and PEO in the bicomponent fibers was studied by comparing their FT-IR and DSC with those of the single-component fibers. The FT-IR spectrum of the CA fibers had a strong ester carbonyl stretching vibration at 1755 cm^{-1}; while that of the PEO fibers exhibited strong peaks around 950 cm^{-1} and 842 cm^{-1}, both are attributed to the C–H out-of-plane deformation vibration in the $–CH_2—CH_2—O—$unit. In the FT-IR spectrum of 30/70 CA (60 kDa)/PEO (600 kDa) bicomponent fibers, both CA and PEO characteristic peaks remained the same as observed in their single-component counterparts (Fig. 11), suggesting little or no interaction between CA and PEO in the bicomponent fibers.

The DSC of all bicomponent fibers with equal mass of CA and PEO from either DMF or 1:1 DMF/dioxane exhibited PEO melting in the 60–67 °C range with heat of fusion values between 74 and 128 J per gram of PEO (Table 2). The existence of crystalline PEO in these bicom-

Table 2
Melting behavior of PEO in 50/50 CA/PEO bicomponent fibers

Molecular weight (kDa)		$T_{m,PEO}$/°C		$\Delta H_{m,PEO}$/(J/g PEO)	
CA	PEO	DMF	1:1 DMF/dioxane	DMF	1:1 DMF/dioxane
30	100	61.2	64.1	−111	−104
30	600	66.7	66.0	−117	−74
60	10	61.9	64.5	−102	−123
60	600	63.2	60.3	−128	−84

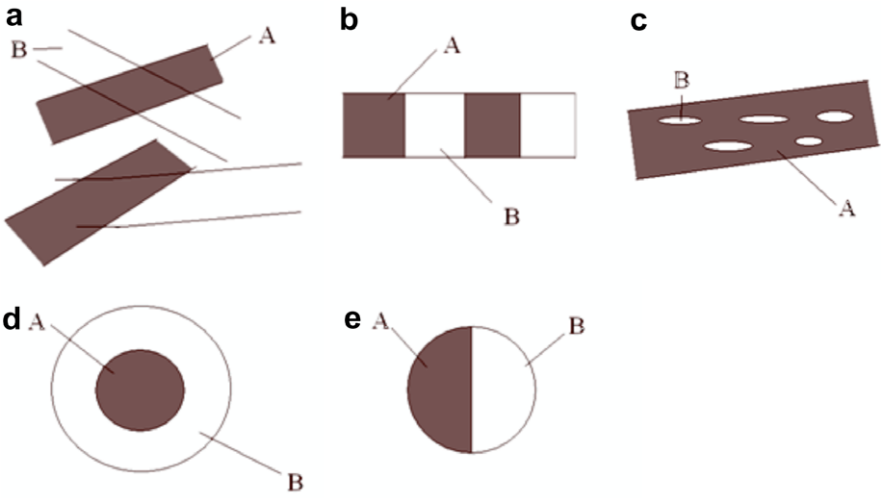

Fig. 12. Schematic models of CA/PEO phase distribution in bicomponent fibers.

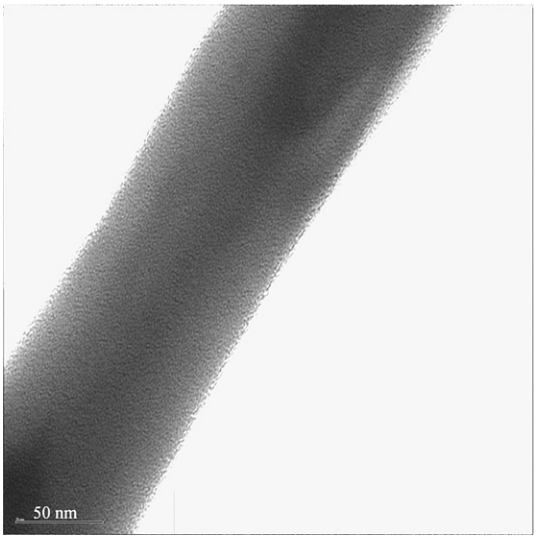

Fig. 13. Water treated (40 °C, 48 h) 30/70 CA (30 kDa)/PEO (600 kDa) fibers from 10% DMF solution (TEM, 50 nm bar).

ponent fibers gives clear evidence that some PEO, if not all, was phase-separated from CA.

Both polymer chain length and solvent system appeared to have influence over the extent of crystallization. The highest T_m and ΔH_m of the 600 kDa PEO were observed in the bicomponent fibers electrospun from DMF, showing crystallization of the long chain PEO was more favorable from DMF. Mixing shorter CA chains with 600 kDa PEO also allowed the formation of larger or more perfect PEO crystals, but not overall crystallinity. Dioxane did, however, improve the crystallization of shorter 10 kDa and 100 kDa PEO chains in the bicomponent fibers. The melting data indicated that PEO phase-separated effectively from CA and the size and extent of the phase-separated PEO domains were more favorable when solvent and chain lengths were properly matched.

In the mixing theory of polymer melts, more distinct polymer–polymer phase separation and larger phase domains are expected in the mixture of high molecular

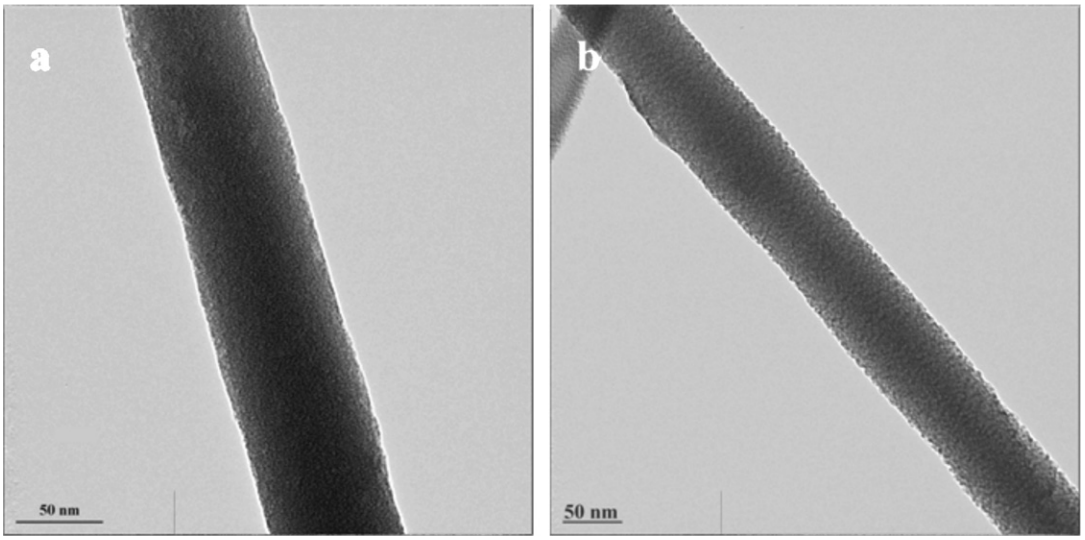

Fig. 14. 50/50 CA (60 kDa)/PEO (10 kDa) fibers from 20% 1:1 DMF/dioxane solution (TEM, 50 nm bar): (a) as-spun; (b) water-treated (40 °C, 4 h).

weight polymers (Folkes & Hope, 1993; He, Chen, & Dong, 1990). With DMF as solvent, the thermal behavior of the bicomponent fibers with either 30 kDa or 60 kDa CA are generally consistent with this theory, i.e., higher T_m and ΔH_m of PEO were observed at higher molecular weight of 600 kDa PEO than those at 100 kDa or 10 kDa. When the more evaporative dioxane was added to DMF, the thermal data do not seem to follow, however. The longest PEO (600 kDa) gave the lowest T_m (60.3 °C) when electrospun with 60 kDa CA from 1:1 DMF/dioxane solution. This deviation may be due to the faster evaporation of dioxane that does not allow CA and PEO to phase-separate into equilibrium state as described in the theory.

3.4. Bicomponent fiber structure

Dissolution of PEO from bicomponent fibers were conducted in distilled water at 40 °C for 4 h. Following such treatment, the bicomponent fibers that contained 70% PEO (600 kDa) had FT-IR spectrum nearly identical to that of pure CA (Fig. 11). The characteristic peak of PEO at 950 cm^{-1} was hardly observed. The 66.1% mass loss from the water treatment was close to the 70% PEO content in the original bicomponent fibers. We have previously shown that as low as 1% PEO in PAN/PEO cast film can be detected by FT-IR (Zhang & Hsieh, 2006). Both the FT-IR spectrum and mass loss value showed that

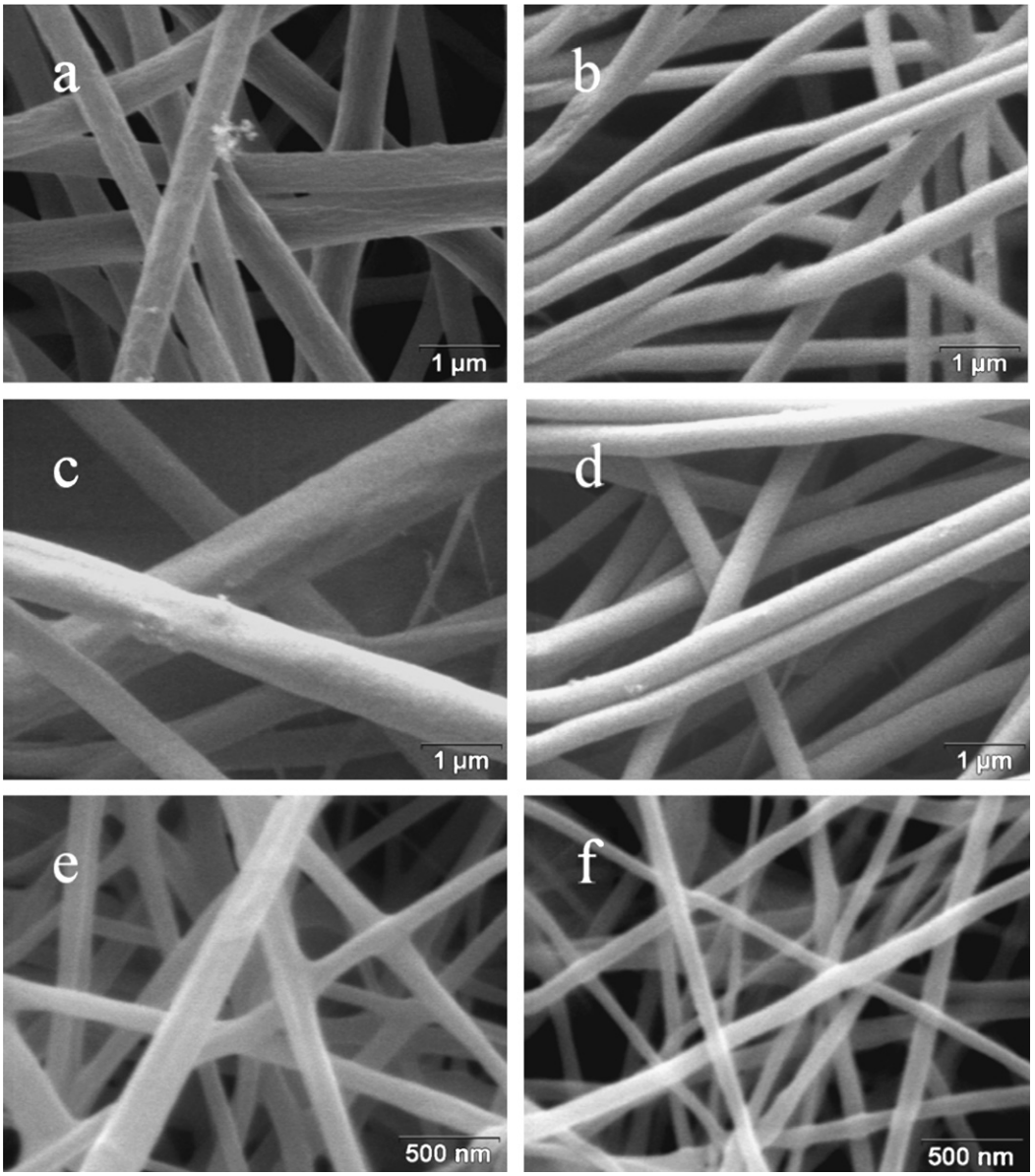

Fig. 15. Size changes of 50/50 CA/PEO bicomponent fibers after water treatment (40 °C, 4 h): CA (30 kDa)/PEO (600 kDa), 10% DMF (a) as-spun; (b) water treated; CA (30 kDa)/PEO (600 kDa), 10% 1:1 DMF/dioxane (c) as-spun; (d) water treated; CA (60 kDa)/PEO (10 kDa), 20% 1:1 DMF/dioxane (e) as-spun; (f) water treated.

Table 3
Diameters of 50/50 CA/PEO bicomponent fibers after water treatment

CA (kDa)	PEO (kDa)	Solvent	Average fiber diameter (nm)		Fiber diameter ratio (water-treated: as-spun)	
			as-spun	Water treated	Experimental	Calculated[a]
30	600	DMF[b]	520 ± 120	315 ± 70	0.61	0.69
30	600	1:1 DMF/dioxane[b]	690 ± 220	430 ± 90	0.62	0.69
60	10	1:1 DMF/dioxane[c]	140 ± 60	95 ± 25	0.66	0.67

[a] Calculation based on equal mass of CA and PEO in sheath–core structure.
[b] 10% Concentration.
[c] 20% Concentration.

600 kDa PEO was almost completely removed from bicomponent fibers under the prescribed condition. For bicomponent fibers containing PEO of lower molecular weight (10 kDa and 100 kDa) and/or at lower proportion (30% and 50%), the removal of PEO is expected to be more efficient and complete.

Both DSC and FT-IR data gave clear evidence of phase-separation between CA and PEO in the bicomponent fibers. In theory, CA and PEO may phase-separate as individual single-component fibers (Fig. 12a) or as co-existed bicomponent fibers (Fig. 12b–e). Fiber morphology and sizes of CA/PEO bicomponent fibers after extended exposure to water were thus examined to help to elucidate the phase-separation form. Upon water treatment of the 30/70 CA (30 kDa)/PEO (600 kDa) bicomponent fibers, the remaining fibers retained their cylindrical shapes (Fig. 13). Similarly, the water treated 50/50 CA (60 kDa)/PEO (10 kDa) bicomponent fibers also kept their shapes (Fig. 14). In both cases, shape retention of fibers indicated that CA exists as continuous phase in the bicomponent fibers. These observations support the phase-separation structures of CA/PEO shown in Fig. 12a, c or d. Furthermore, bicomponent fibers showed significant size reduction following water treatment (Fig. 15 and Table 3). In fact, the experimentally determined diameter ratios of bicomponent fibers before and after water treatment showed excellent matches with the calculated values of the CA core and PEO sheath structure (Fig. 12d). This finding is distinctively different from PAN/PEO bicomponent fibers, where PEO was dispersed in PAN matrix as an island-in-the-sea structure as shown in Fig. 12c (Zhang & Hsieh, 2006). The difference in their phase separation structures is attributed to the difference in molecular flexibility between the polymer pairs. PEO molecular chains are highly flexible but the CA backbone is much more rigid than the PAN chains. Such difference in molecular flexibility is even larger between the longer CA and shorter PEO, thus facilitated the formation of ideal sheath–core structure. The perfect match of experimental fiber diameter ratios with theoretical values in the case of 50/50 CA (60 kDa)/PEO (10 kDa) gave strong support for this structure (Table 3).

4. Conclusion

The formation and structure of CA/PEO bicomponent fibers were investigated by electrospinning of binary mixtures of these two polymers. The threshold molecular weights of CA and PEO to support fiber formation from electrospinning of 20% solutions in DMF were 50 kDa and 100 kDa, respectively. Fiber formation improved with longer polymer chain lengths of 60 kDa CA and 600 kDa PEO. Increasing total polymer concentrations from 5 to 30 wt% also improved fiber formation by enhancing chain entanglement, while also led to larger fibers. Adding the low dielectric constant dioxane as a co-solvent enabled electrospinning of the 30 kDa CA into uniform fibers by reducing the electrical stretching force on polymer jet. With the binary CA/PEO mixtures, longer chain lengths of either polymer enabled bicomponent fiber formation at lower total polymer concentrations, but led to larger fiber sizes. Even with the non-fiber-forming 10 kDa PEO, either dioxane addition or reduced PEO content facilitated bicomponent fiber formation. Clear phase separation between CA and PEO in the bicomponent fibers was supported by the lack of interference of FT-IR characteristic peaks of either polymer and well defined PEO melting from DSC. Upon dissolution of PEO by water, the fibers retained their cylindrical shape and smooth surfaces. The diameter reduction was comparable to the PEO content, supporting the notion that the bicomponent fibers had a CA core and PEO sheath structure. Such sheath–core structure was more prominent with the longer CA (60 kDa) and shorter PEO (10 kDa) pair that had the most distinctively different molecular flexibility.

Acknowledgements

This work was supported by the National Textile Center, USA (C04-CD06s) and Jastro-Shields Graduate Research Award from University of California, Davis.

References

Brandrup, J., Immergut, E. H., & Grulke, E. A. (1999). *Polymer handbook* (4th ed.). New York: Wiley.

Creton, C., Kramer, E. J., & Hadziioannou, G. (1991). Critical molecular weight for block copolymer reinforcement of interfaces in a two-phase polymer blend. *Macromolecules, 24*(8), 1846–1853.

Demir, M. M., Yilgor, I., Yilgor, E., & Erman, B. (2002). Electrospinning of polyurethane fibers. *Polymer, 43*(11), 3303–3309.

Ding, B., Kimura, E., Sato, T., Fujita, S., & Shiratori, S. (2004). Fabrication of blend biodegradable nanofibrous nonwoven mats via multi-jet electrospinning. *Polymer, 45*(6), 1895–1902.

Doshi, J., & Reneker, D. H. (1995). Electrospinning process and applications of electrospun fibers. *Journal of Electrostatics, 35*(2–3), 151–160.

Folkes, M. J., & Hope, P. S. (1993). *Polymer blends and alloys*. Glasgow: Blackie Academic & Professional.

He, M. J., Chen, W. X., & Dong, X. X. (1990). *Polymer physics*. Shanghai: Fudan University Press.

Inoue, T., Ougizawa, T., Yasuda, O., & Miyasaka, K. (1985). Development of modulated structure during solution casting of polymer blends. *Macromolecules, 18*(1), 57–63.

Kim, C.-W., Frey, M. W., Marquez, M., & Joo, Y. L. (2005). Preparation of submicron-scale, electrospun cellulose fibers via direct dissolution. *Journal of Polymer Science Part B: Polymer Physics, 43*(13), 1673–1683.

Kulpinski, P. (2005). Cellulose nanofibers prepared by the *N*-methylmorpholine-*N*-oxide method. *Journal of Applied Polymer Science, 98*(4), 1855–1859.

Li, L., & Hsieh, Y.-L. (2006). Chitosan bicomponent nanofibers and nanoporous fibers. *Carbohydrate Research, 341*(3), 374–381.

Li, L., & Hsieh, Y.-L. (2005a). Ultra-fine polyelectrolyte fibers from electrospinning of poly(acrylic acid). *Polymer, 46*(14), 5133–5139.

Li, L., & Hsieh, Y.-L. (2005b). Ultra-fine polyelectrolyte hydrogel fibers from poly(acrylic acid)/poly(vinyl alcohol). *Nanotechnology, 16*(12), 2852–2860.

Li, M., Guo, Y., Wei, Y., MacDiarmid, A. G., & Lelkes, P. I. (2006). *Biomaterials, 27*(13), 2705–2715.

Liu, H., & Hsieh, Y.-L. (2002). Ultrafine fibrous cellulose membranes from electrospinning of cellulose acetate. *Journal of Polymer Science Part B: Polymer Physics, 40*(18), 2119–2129.

McKee, M. G., Wilkes, G. L., Colby, R. H., & Long, T. E. (2004). Correlations of solution rheology with electrospun fiber formation of linear and branched polyesters. *Macromolecules, 37*(5), 1760–1767.

Reneker, D. H., & Chun, I. (1996). Nanometre diameter fibres of polymer, produced by electrospinning. *Nanotechnology, 7*(3), 216–223.

Son, W. K., Youk, J. H., Lee, T. S., & Park, W. H. (2004a). Preparation of antimicrobial ultrafine cellulose acetate fibers with silver nanoparticles. *Macromolecular Rapid Communications, 25*(18), 1632–1637.

Son, W. K., Youk, J. H., Lee, T. S., & Park, W. H. (2004b). The effects of solution properties and polyelectrolyte on electrospinning of ultrafine poly(ethylene oxide) fibers. *Polymer, 45*(9), 2959–2966.

Subbiah, T., Bhat, G. S., Tock, R. W., Parameswaran, S., & Ramkumar, S. S. (2005). Electrospinning of nanofibers. *Journal of Applied Polymer Science, 96*(2), 557–569.

Sun, Z., Zussman, E., Yarin, A. L., Wendorff, J. H., & Greiner, A. (2003). Compound core-shell polymer nanofibers by co-electrospinning. *Advanced Materials, 15*(22), 1929–1932.

Xie, J., & Hsieh, Y.-L. (2003). Ultra-high surface fibrous membranes from electrospinning of natural proteins: Casein and lipase enzyme. *Journal of Materials Science, 38*(10), 2125–2133.

Zhang, L., & Hsieh, Y.-L. (2006). Nanoporous ultrahigh specific surface polyacrylonitrile fibres. *Nanotechnology, 17*(17), 4416–4423.